Chapter 13
The Manufacturing of Natural Fibre-Reinforced Composites by Resin-Transfer Molding Process

Deepak Verma

Abstract Natural fibre composites became a most important and versatile theme of research. This area/theme not only utilizes the agricultural wastes such as rice husk, bagasse fibres, banana fibres, etc. but also provides a new material made from these wastes which are light in weight, have low cost, and have high mechanical strength. Nowadays, there are so many methods available for the processing or fabrication of polymer composites. Some of these methods are hand layup method, injection molding method, compression molding, spray-up method, resin-transfer molding (RTM), etc. In this chapter, we are specifically discussing about the RTM process and their important parameters for manufacturing of the polymer composites. Various mechanical properties and characterization of composite materials made by RTM have also been discussed and reported here.

Keywords Polymer composites • Resin-transfer molding • Mechanical properties • Morphological study

13.1 Introduction

The resin-transfer molding (RTM) is one of the most important technologies available for composite making. The capability of RTM process is seen in making of large complex three-dimensional part having great dimensional variation and good surface finish. Better scheme of RTM process fabricates 3-D complicated parts and offered fabrication of low value structural parts in average amounts. The RTM process is generally known as cost-effective manufacturing method for the fabrication of composites. In RTM method, a catalyzed thermosetting resin is injected into an

D. Verma (✉)
Department of Mechanical Engineering,
Graphic Era Hill University,
Dehradun, Uttarakhand 248001, India
e-mail: dverma.mech@gmail.com

M.S. Salit et al. (eds.), *Manufacturing of Natural Fibre Reinforced Polymer Composites*, DOI 10.1007/978-3-319-07944-8_13

enclosed metal mold which contains a reinforcement preform. The preform is compressed to the defined fibre volume fraction when the matched mold is closed. The mold is filled with resin, and fibres become wet at that time and curing takes place inside the mold. There are some benefits of RTM on various available composite making processes; some of these are autoclave molding, compression molding, etc. RTM process is generally considered as a closed mold process which ultimately lowers the worker's subjection to detrimental volatiles, like styrene, and relates room temperature processing resins. Nevertheless, RTM process is a costly process and the tool design becomes arduous when manufacturing large and complicated shaped parts.

RTM manufactured continuous fibre-reinforced composite. RTM distinctly reduces the manufacturing cycle times as compared to other available composite making methods, and it is a feasible method for mass production of composites parts.

13.2 Detailed Study of RTM Process

The RTM process generally used a stiff closed mold. Figure 13.1 shows the RTM process sequence by considering easy case. A half mold is used in this process to arrange the preform. After this, close the mold and compress the preform. Then, introduce the resin into the mold by using positive gradient pressure which ultimately replaces the air entrapped into the preform. Vacuum is also utilized at some exclusive vents and removes the entrapped air from the mold. The preform is impregnated by the resin into the mold. After that, the curing of composite is considered to start. The next and last step is to open the mold and remove the part from it. The mold closing sequence is distinguished by the compression of the reinforced fibre which permits to have the appropriate thickness. The compression changes the microstructure of the preform, developing substantial distortions and nonlinear viscoelastic effects. These effects show changes in energy of the material and generated stresses (residual or leftover) just because of the viscoelastic response of the fibres. Still, stresses released throughout the impregnation phase. The introduction of resin assured the entire impregnation of the preform, whereas in general poor

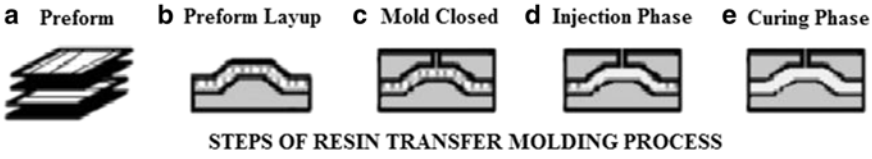

Fig. 13.1 Sequence of the main steps of RTM process. (**a**) realization of the preform, (**b**) deposition and draping of the preform in the mold cavity, (**c**) closing mold, (**d**) injection phase, and (**e**) curing phase

impregnation of the fibres gives dry spots with disordered adherence between the layers which ultimately make the surface rough and irregular (Laurenzi and Marchetti 2012).

13.2.1 Important Components of RTM Process

There are five important components in the RTM process.

1. Resin and catalyst container
2. Pumping unit
3. Mixing chamber
4. Resin injector
5. Molding unit

Two separate containers are to be taken for the resin and catalyst. The resin container should be bigger in contrast to the catalyst container. Both of the containers pass through the pumping unit having separate outlets which goes to the mixing chamber. The purpose of the pumping unit is to transfer and mix both of the resin and catalyst in the mixing chamber. This mixture is introduced into the mold cavity by resin injectors. The molding unit consists of upper half and lower half molds. Generally, heating systems are attached with the molding unit. Some vents are provided into the mold cavity to release the entrapped gases during clamping.

13.3 Components Made by RTM Process

The RTM process generally uses two main materials for the fabrication of composites; these are reinforcement and resin. The RTM process used a vast range of various reinforcement and resin systems for the manufacturing of a composite material with a wide range of properties. The important parameter generally considered for the designing of a composite product is the good understanding of the raw material properties as it has been considered that each fibre and resin system has their individual contribution for making the composites. The main aim of the reinforcement is to provide good mechanical properties like stiffness, tensile strength, and impact strength, whereas on the other side the resin system provides physical properties to the composite in addition to the resistance to corrosion, fire, etc. and also gives some rigidity which is important from the solid composite point of view.

The performance and the process of composite design are affected by the reinforcing materials such as the choice of the fibres (for reinforcement) and fibre structure. Fibre selection depends upon the performance like modulus, strength, durability, compressibility, and adequate volume fractions for the proper placement of the reinforced material during preforming operations.

13.4 Selection of Important Parameters for RTM Process

There are some variables and parameters available in RTM process which are dependent on each other. The combination of both of the variables and parameters influences not only the process but also the quality and finishing of the product. Therefore, they should be thoroughly determined. Pressure, temperature, viscosity, and volume fraction are some of the significant parameters which cannot be omitted in design of the composite material. The other parameters that should be taken into account are the angle of strike of the nozzle, the fibres placement, the flow route and shear rates, etc. It has been observed that the resin flows swiftly in the direction of the fibres; thus, the flow movement is generally based upon the kind of fabric used and the number of overlapped layers. For the attainment of the homogeneous distribution of the resin, it is essential to have an accurate number of skins.

13.4.1 Thickness

The thickness is also another parameter. If the thickness is not considered under specified limit, then it may cause the formation of the voids and dry spots on the composite and also influence the flow progress and impregnation of the fibres. The thickness becomes a crucial design requirement specifically in the instance of the addition of reinforcements and ribs.

13.4.2 Injection Pressure

The injection pressure is another important parameter which not only evaluates the velocity of the resin which enters in to the mold but also the hydraulic pressure of the mold. Generally, the entering velocity elucidates the pouring time. The pouring time should not be less. If it is less, then it results not only in an inadequate impregnation of the fibres but also in the similar time untimely gelation of the resin occurred. The injection pressure generally related to the dispersion of the resin on the preform. If the dispersion of resin is not uniform, then it results in the formation of air bubbles in the matrix which ultimately affects the surface quality and the mechanical properties of the composite. This parameter also has some importance with the viscosity term called “fibre wash.” The fibres can move directly under the injection pressure if the binder mixed too rapidly in contact with the resin.

13.4.3 Temperature

The temperature is also an exceptionally significant parameter and factually associated with the injection pressure and the resin viscosity. The increase in temperature results in the decrease in pouring time which ultimately lowers the pressure.

Similarly, a decrease in temperature results in an increase in the viscosity which results in an increase in the pressure to confirm the transport of the resin itself.

13.5 Influence of RTM Process on Final Product

The quality and the performance of the product mainly depend on the process used for the fabrication. For example, if the composite has a good surface finish, then it ultimately gives the better mechanical properties. A good surface finish averts the inclusion of the elements like dust which produces and intensifies the micro-cracks inside the structure resulting in lower mechanical properties. Figure 13.2 demonstrates the steps of the process that affect the response of material and define the connection among the process and conclusive implementation. The two stages, viz., compaction and impregnation stages, control the imperfections due to voids and dry spots. These can be defined as follows.

13.5.1 Compaction Stage

For the fabrication of the advanced composite materials, the compaction stage plays an important role. This stage generally appears by the use of an external pressure, which makes disposition of the fibres and alteration of microstructure. In RTM, the compaction phase takes place by closing the mold which results in the attainment of the fibre volume fraction by the preform. The large numbers of distortions in the preform are generally observed in the compaction phase. This only happened by a variation in energy observed in the material. For example, when a compaction of multilayer preform is taking place, the fibres move and flatten with other fibres, thus producing interlayer nesting phenomena which depend on the failure mode and the

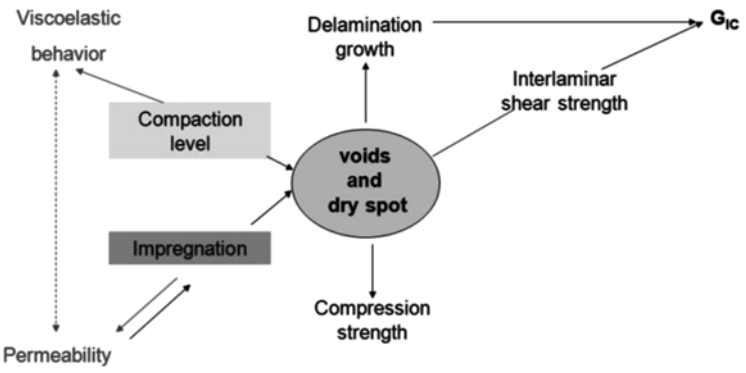

Fig. 13.2 Relations between manufacturing phases and material behavior (Laurenzi and Marchetti 2012)

fibres' structure. After removal of the compression load, fibres do not return to their original position inside the preform.

If there will be any changes like mechanical and spatial changes in the preform, which modifies the mechanical properties of the composite materials, then it generally refers to the phenomenon of nesting. Specifically, the nesting affects the rigidity and resistance of the piece. Certainly, the stiffness is based on the placing of the layers. If the layer is set without any reduction in the thickness, then there is no significant change noticed in any mechanical properties.

13.5.2 Impregnation Phase

The voids formation and dry spots are the defects induced by the RTM process and become the major problems which affect the production quality of the product. The voids cause the failure of the matrix material. The mechanism of crack formation is generally seen in composites by the emergence of micro-voids among fibres which ultimately results in the delamination of the composites. The two resistance levels by preform are observed in the resin flow, i.e., between the fibre bundles and inside the fibre bundles. This ultimately can be understood by the two different permeabilities, i.e., the permeability between the fibre bundles and inside the fibre bundles. The kind of flow scale intent the void formation in composites. The phenomenon of emergence of macro-voids in the macroscale can be observed when the displaced air remains trapped in the resin system or, on the other hand, when inadequate pressure overcomes the resistance of the preform. In case of microscale, micro-voids generally result or give rise to porosity. The general mechanism of emergence of voids in fibre bundles can be shown in Fig. 13.3. The mechanism states that the flow front flows around the tows and continues to impregnate the tow after the passage of the front. If the trapped air (in tow) is not deported during the start of the pouring process, then it ultimately results in the generation of the micro-voids at the center. Macroscopic pressure drop is another reason of the formation of micro-voids. The

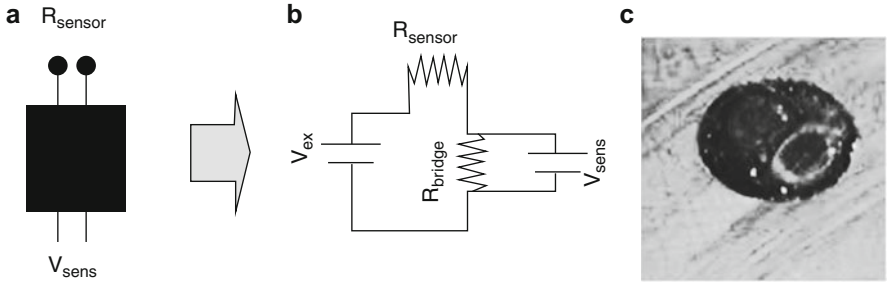

Fig. 13.3 Mold embedded dielectric point sensor: (**a**) schematic, (**b**) circuit diagram, and (**c**) photograph. Lawrence et al. (2002) (Reproduced with permission from Elsevier Ltd.)

pressure drop offers an observable change in the permeability along the preform and can be justified by the sink effect. In this, the fibre bundles generally considered as fluid sinks. In this, the fibres of the bundle are placed much closer than that existing between two bundles. In the same time, the flow of resin takes place between the fibre bundles. This ultimately results in the impregnation of the bundle (Laurenzi and Marchetti 2012).

13.6 RTM Composites: A Past Research

Lawrence et al. (2002) developed a design and control methodology for mold filling by simulation by using some sensors and actuators. This recognizes the distraction of flow in the mold filling process and directs the resin to successfully flow into the mold without formation of voids. This technique is applied and approved for a mold geometry which generally has the complicated features such as tapered regions and thick regions. The position of the sensors in the mold can be observed by the application of software tools. These tools noticed the expected distraction and recommend flow control actions for additional actuators to redirect the flow. Laboratory hardware is used for the automation of the pouring process. These sensors control the flow of the resin and impregnate all the fibres completely against the distraction in the process.

The point sensor senses the resin in significant locations. From a manufacturing point of view, the sensors are the combined part of the tooling. The data acquisition system was used to connect the sensors. The small current flow was used to determine the presence of resin when it wets the two poles of the sensor. The half bridge setup was used to detect the current excited by a 10 VDC power supply incorporated in the data acquisition system as shown in Fig. 13.3.

Leclerc and Ruiz (2008) carried out an experimental analysis on various kinds of fibrous reinforcements for the optimal analysis of the impregnation conditions in relation to the content of macro-/micro-voids to the local capillary number. The effect of voids on the mechanical properties of the laminates was also studied. From Fig. 13.4, it is noticed that the macro-voids generally evolved at less speed during fibre impregnation. This is only because of the capillary action, and they can overreach 15 % in volume. The reason behind the micro-void formation pertains to the high velocity of the resin, but at a very less rate (approx. 2 % in volume). From this, it can be observed that the resin impregnation velocity has some critical value, and it should not fall below this. Figure 13.4 shows an optimum impregnation velocity which ultimately results in minimum void formation.

Hsiao and Gangireddy (2008) used a vacuum-assisted resin-transfer molding (VARTM) process which infuses a little quantity of carbon nanofibres with resin into the glass fibre preform which ultimately controls and decreases the spring-in angle. From these results, it can be observed that the carbon nanofibres totally restrained the spring-in angle of L-shaped composites. These spring-in angles were measured only after being de-molded. Figure 13.5 represents and differentiates the

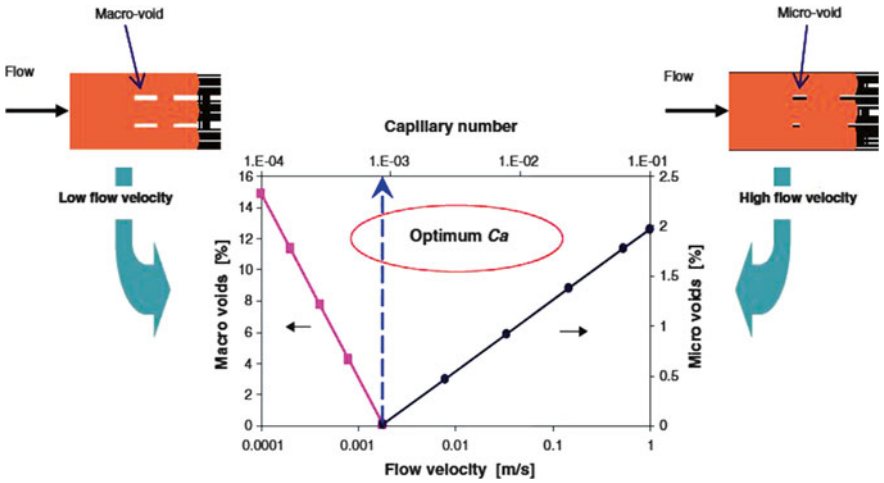

Fig. 13.4 Macroscopic and microscopic void formation during fibre impregnation related to the flow velocity and capillary number (Ca). An optimum Ca corresponds to minimum void [5]. Leclerc and Ruiz (2008) (Reproduced with permission from Elsevier Ltd.)

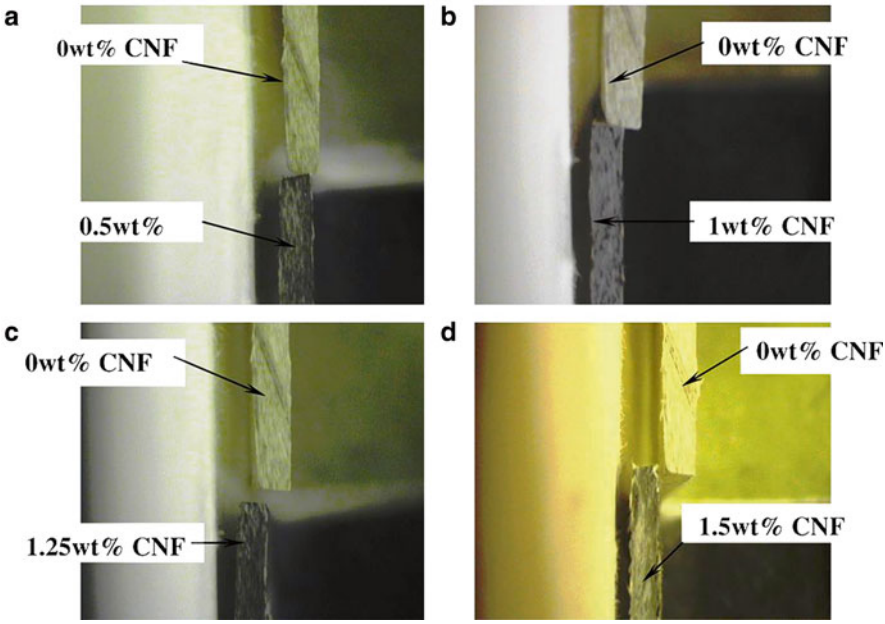

Fig. 13.5 Top-view comparison of the spring-in between the control sample and the samples with various CNF weight fractions. (**a**) 0 and 0.5 wt% CNF specimens. (**b**) 0 and 1 wt% CNF specimens. (**c**) 0 and 1.25 wt% CNF specimens. (**d**) 0 and 1.5 wt% CNF specimens. Hsiao et al. (Reproduced with permission from Elsevier Ltd.)

Table 13.1 Experimental data for the L-shaped composite specimens (Hsiao and Gangireddy 2008) (Reproduced with permission from Elsevier Ltd.)

	0 wt%	0.5 wt%	1 wt%	1.25 wt%	1.5 wt%
Room temperature	20.1	21.4	21.0	21.5	21.1
ΔT_{top} (°C)	−10.2	−8.0	−6.4	−4.8	−6.4
ΔT_{mid} (°C)	−10.8	−8.3	−6.0	−5.6	−6.4
ΔT_{bottom} (°C)	−11.6	−8.1	−6.4	−5.6	−5.9
$\Delta t_{average}$ (°C)	−10.9	−8.1	−6.4	−5.6	−5.9
Spring-in angle (°)	2.340±0.318	1.830±0.318	1.330±0.318	0.972±0.318	0.634±0.318

spring-in effects of the various L-shaped composites of 0, 0.5, 1, 1.25, and 1.5 wt% carbon nanofibre weight fractions.

The L-shaped samples were observed from the top. These samples were placed in a 90° bracket with their base sides fixed. Figure 13.5 represents that the 0 wt% carbon nanofibre part has the highest spring-in distortion as compared to the composite parts having some fractions of CNFs in the matrix. The composite having CNF's percentage of 1.5 wt% has the lowest spring-in distortion in contrast to the other available specimens. Table 13.1 shows the measured spring-in angles for the L-shaped parts. The temperature information is also showed in Table 13.1 during the cure process. It has been observed from Table 13.1 and Fig. 13.5 that the spring-in angles of the L-shaped composite part decrease noticeably by increasing the wt% fraction of carbon nanofibres in the matrix.

Sreekumar et al. (2012) studied the electrical properties of sisal fibre-reinforced polyester composites manufactured by RTM process by considering fibre loading, frequency, and temperature. From the study, it has been found that the dielectric constant (ε'), loss factor (ε''), dissipation factor (tan δ), and conductivity increase by increasing the fibre content for all range of frequencies. From these results, it has been noticed that the values are found maximum for composites with fibre content of 50 vol.%. The volume resistivity also varied with fibre loading at smaller frequency. The increase in temperature ultimately improves the dielectric constant values by decreasing the glass transition temperature. This variation is only because of the fibre content.

Figure 13.6 shows the variation of the dielectric constant of sisal/polyester composites as a function of frequency. From Fig. 13.6, it has been observed that the dielectric constant increases by increasing fibre content on all range of frequencies such as polyester<R20<R30<R40<R50. The ε' values primarily based upon the effects of interfacial, orientation, atomic, and electronic polarizations in the material. The interfacial polarization occurs just because of the differences in conductivities. The orientation and interfacial polarizations also depend on the concentration of fillers. The available polar groups in the natural fibres have resulted in an important increment in ε' value by increasing the fibre loading. This can be understood by Fig. 13.7 showed the variation of the ratio between dielectric constant of composites and matrix behaving as a function of fibre content. In case of polyester, the

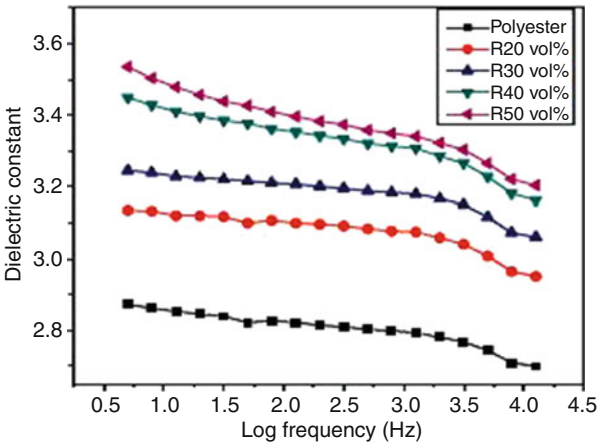

Fig. 13.6 Variation of dielectric constant of sisal/polyester composites as function of fibre content and frequency at 30 °C (Reproduced with permission from Elsevier Ltd.)

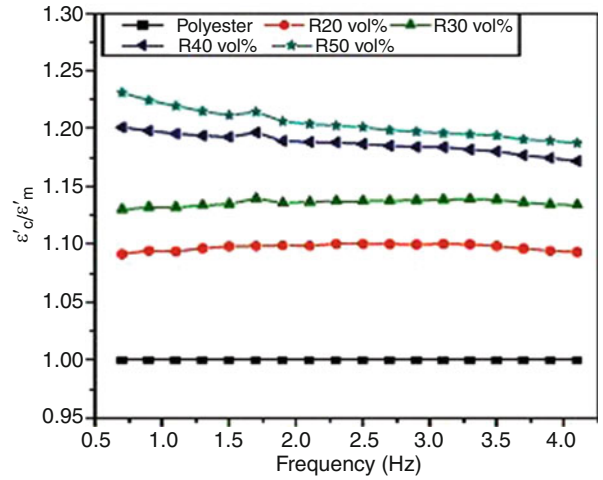

Fig. 13.7 Plot of ratio of dielectric constant of composites with that of matrix as a function of fibre content at 30 °C (Reproduced with permission from Elsevier Ltd.)

ε′ value is low because it has only momentary atomic and electronic polarizations. On the other hand, it is noticed that for a stated fibre loading, the ε′ gives maximum values at low frequencies. This is because of the reduction in the orientation polarization with increased frequency. Loss factor (ε″) is the average power factor over a given period of time which describes the losses in transmission and distribution. The variation of ε″ for the composites is shown in Fig. 13.8. It can be noticed that ε″ is high in lower frequency region and is found maximum for the composites with a fibre content of 50 vol.%. By increasing the frequency, the value of ε″ decreases rapidly. The dissipation factor (function of frequency) at various fibre loadings is shown in Fig. 13.9. This dissipation factor decreases by increasing the frequency. It has been noticed that increasing the fibre content in the low frequency region represents a significant variation, i.e., it is minimum for polyester and maximum for R50

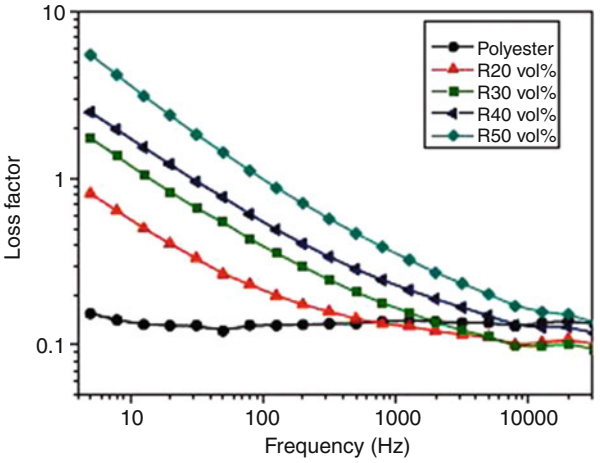

Fig. 13.8 Variation of loss factor of sisal/polyester composites as function of frequency at 30 °C (Reproduced with permission from Elsevier Ltd.)

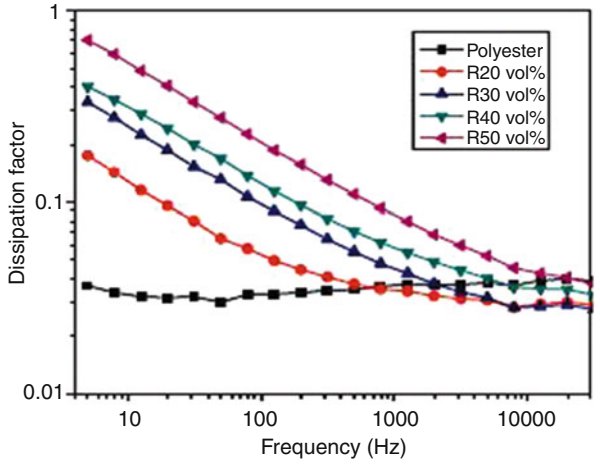

Fig. 13.9 Variation of dissipation factor of sisal/polyester composites as a function of frequency at 30 °C (from paper Sreekumar et al. 2012) (Reproduced with permission from Elsevier Ltd.)

for a given range of frequency. On the other hand, in higher frequency range, tan δ curves come nearer as seen in the loss factor. Also increasing the fibre content results in an increase in the number of polar groups which again increases the orientation polarization which results in an improvement in the dissipation factor.

Pearce et al. (1998) fabricated different types of carbon/epoxy plates by RTM. The plates were fabricated by using the same fabrics, and then it sends for microstructural image analysis and interlaminar shear strength (ILSS) testing according to CRAG standards. Quantimet 570 automatic image analyzer was used to measure some relationships between measured permeabilities and finished microstructures.

Schmachtenberg et al. (2005) used and applied ultrasonic techniques for online monitoring and controlling of RTM. In this study, a master mold was fabricated to

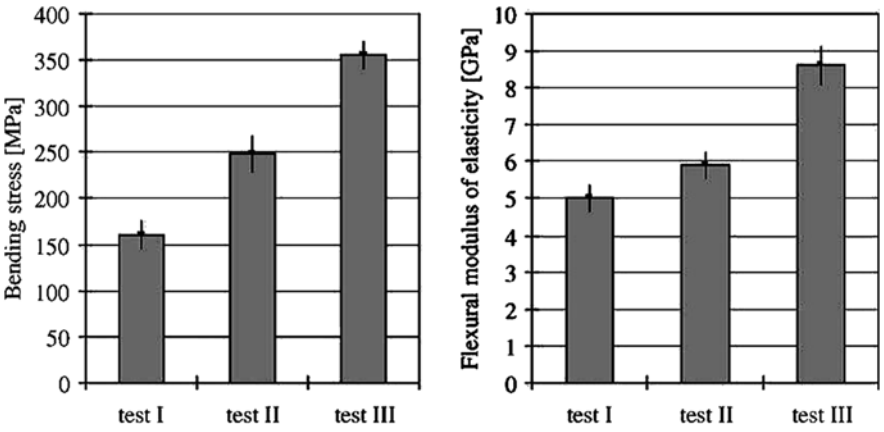

Fig. 13.10 Three-point bending properties of the RTM samples, preform: continuous random mat (Schmachtenberg et al. 2005) (Reproduced with permission from Elsevier Ltd.)

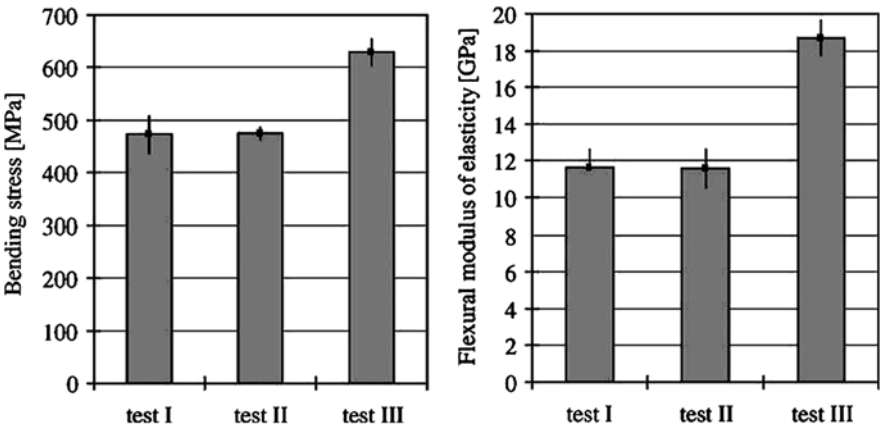

Fig. 13.11 Three-point bending properties of the RTM samples, preform: multiaxial layers (Schmachtenberg et al. 2005) (Reproduced with permission from Elsevier Ltd.)

examine the ultrasonic technique as compared to pressure transducers and dielectric sensors. The main objective of this study was to constrain the flow front during injection and to observe the curing behavior of the resin.

The RTM process is completed with this mold by direct transmission sensors of 8 mm diameter and a frequency of 4 MHz. Firstly, the investigation can be carried out by applying measurement device to the RTM process, and then different types of resin systems were distinguished. After this study, a correlation between different process parameters, ultrasonic signals, and part properties was observed. Three-point bending tests were carried out for the estimation of the mechanical properties of the RTM composites. The bending tests were also carried out on composite laminates.

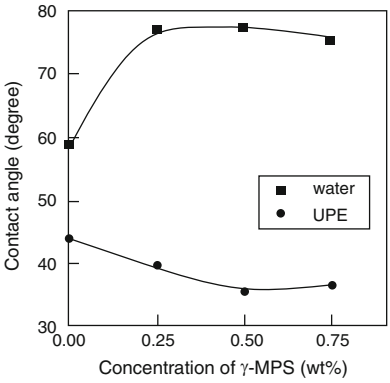

Fig. 13.12 Advancing contact angles of glass plate with the variation of g-MPS treatment concentration. Lee et al. (2002) (Reproduced with permission from Elsevier Ltd.)

The mechanical characteristics of the sample can be shown in Figs. 13.10 and 13.11. From these results, it has been noticed that a correlation between the measured amplitude maxima and the mechanical properties exists. From Fig. 13.10 and 13.11, it can be noticed that by giving variation in the process parameters, the mechanical value of the composite with random mat become doubled.

Lee et al. (2002) investigated the influence of glass fibre surface modification on the flow properties of unsaturated polyester (UPE) resin by the resin-transfer molding process. This g-methacryloxypropyl trimethoxysilane (γ-MPS) was adopted as a glass fibre surface modifier. It has been observed that the γ-MPS treatment decreases the surface energy of glass fibre by advancing the contact-angle measurement. Darcy's law was used for measuring the unsteady state permeability of glass fabric preforms.

Figure 13.12 shows the advancing contact angles of the glass plate in distilled water and UPE resin at various γ-MPS treatment concentrations. In case of water, increasing the concentration of γ-MPS ultimately increases the advancing contact angle and shows a plateau value. On the other hand, the contact angle decreases by dipping the glass plate into UPE resin under the same experimental conditions for water. Figure 13.13 shows the flexural properties of the glass fibre/UPE composites. From Fig. 13.13, it has been noticed that the flexural strength and modulus of γ-MPS-treated glass fibre/UPE composite are higher than those of untreated composites. When the silane coupling agent is used to treat the glass fibre surface, there is a formation of siloxane bond that takes place on the glass fibre surface via a condensation reaction. The improved interfacial adhesion leads to form a chemical bond, at the interface.

Rouison et al. (2004) used RTM process to develop hemp/kenaf fibre/UPE composites. In this research, the fibre mats having a moisture content of 4.3–5 % were dried in the mold under vacuum condition and got the final moisture value of around 1–2 %. The low permeability of the fibre mat ultimately increases the resin injection time at high fibre contents. They keep the temperature of the mold constant to obtain homogeneous curing of the part at fast rate. Figure 13.14 represent the results of

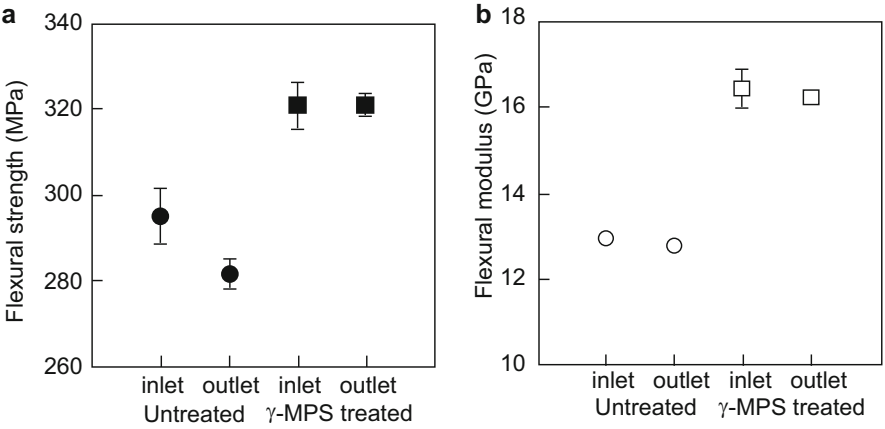

Fig. 13.13 Flexural property of the glass fibre/UPE composites: (**a**) flexural strength and (**b**) flexural modulus (Lee et al. 2002) (Reproduced with permission from Elsevier Ltd.)

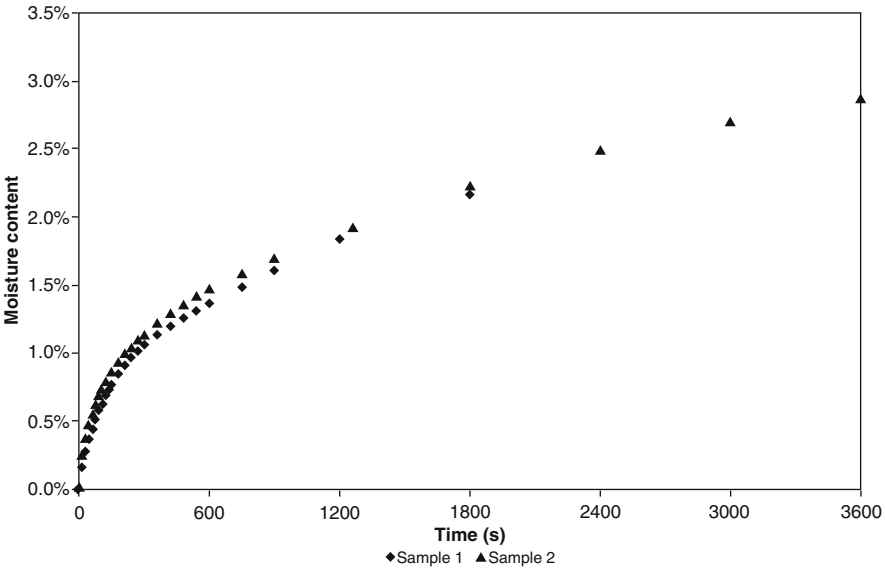

Fig. 13.14 Water absorption rate of the fibres under standard conditions after drying for 2 h at 105 °C (Rouison et al. 2004) (Reproduced with permission from Elsevier Ltd.)

these experiments. From figure, it can be noticed that the moisture content at 50 %RH was only of 4.1 %. The water available in the fibres begins to increase across this point to reach about 12 % at 94 %RH. So for this reason, the fibres were kept in a standard room at 23 °C, 50 % RH permanently because of the variations in

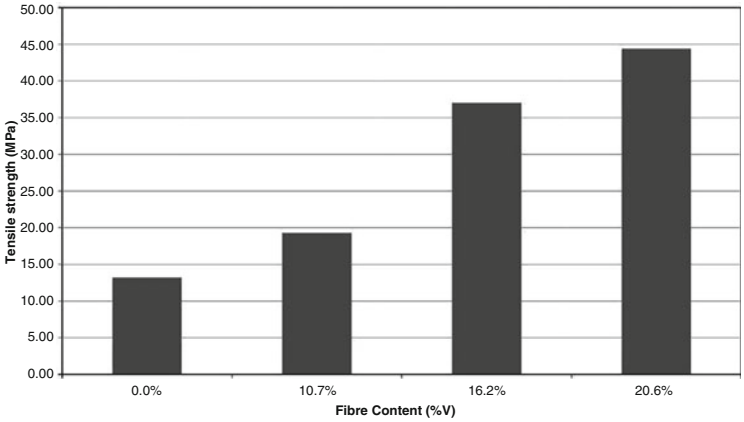

Fig. 13.15 Tensile strength of natural fibre composites (Rouison et al. 2004) (Reproduced with permission from Elsevier Ltd.)

atmospheric conditions. The moisture absorption rate of the fibres after drying at 105 °C for 2 h was also measured.

The tensile strength of the composites is presented in Fig. 13.15. An improvement in the tensile strength of the samples is observed by increasing the fibre content. A considerable improvement was noticed between the pure resin and the sample with 20.6 % fibres, from 13.1 to 44.3 MPa. From these results, it has been found that the tensile strength of composites with 20 % fibres is around 100 MPa, whereas on the other hand the flexural tests of the same composite showed a highest value of 71.4 MPa.

Lin et al. (2006) prepared layered silicate/glass fibre/epoxy hybrid composites by using a VARTM process. In this study, two directions, i.e., parallel and perpendicular to the flow direction of resin, were used, and then the effects of the fibre direction on the clay distribution in the hybrid composites were checked. The morphological study of the composites was investigated by using X-ray diffraction (XRD) and transmission electron microscopy (TEM). The dispersion of clay in the composites was also noticed by using scanning electron microscopy (SEM). The results showed that reinforcing a small amount of organoclay in the glass fibre/epoxy composites ultimately enhances their mechanical and thermal properties.

Three-point bending test was used for the investigation of the flexural properties of the nanocomposites in both directions, i.e., parallel and perpendicular to the fibre alignment. Figure 13.16 shows that reinforcement of clay ultimately increases the transverse flexural modulus of composite. The impact properties of the nanocomposites with various clay loadings are presented in Fig. 13.17. It is observed that the perpendicular impact direction decreases the impact strength with clay loading, while if the impact is along the fibre direction, the impact strength increases by increasing the clay loading.

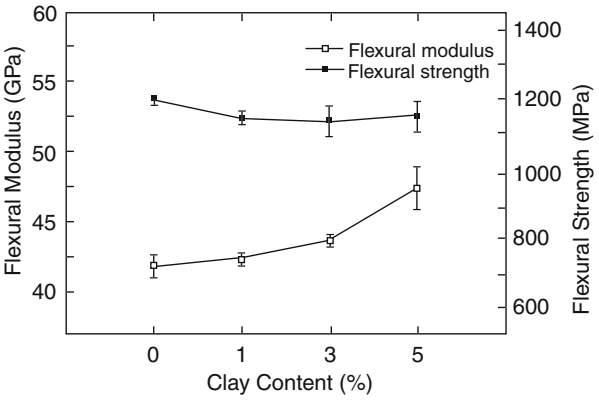

Fig. 13.16 Flexural properties of the nanocomposites with different clay loadings in the fibre direction (Lin et al. 2006) (Reproduced with permission from Elsevier Ltd.)

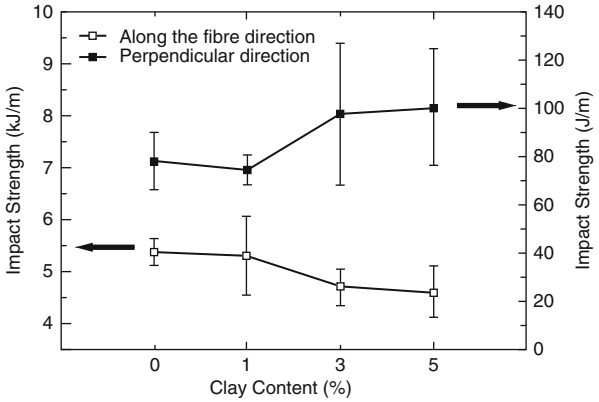

Fig. 13.17 Impact strength of nanocomposites with different clay loadings in two directions (Lin et al. 2006) (Reproduced with permission from Elsevier Ltd.)

Papargyris et al. (2008) incorporated microwave heating in RTM process. About 50 % reductions in cure cycle time were achieved by using microwave heating. The mechanical testing result shows the same values of flexural properties of the two types of composites. Microwave-cured composites observed about 9 % increase of the ILSS. This improvement in ILSS is due to a less resin viscosity at the first stage of the curing process as confirmed by SEM. Again, both kinds of composites yielded less void content (<2 %).

Figure 13.18 shows the viscosity change against time at three different heating rates (2, 5, and 10 °C/min) for the neat LY/HY5052 resin system. By increasing the heating rate, the viscosity of the neat resin decreases considerably from 0.12 to 0.068 Pa s and reached a final value of 0.043 Pa s. Excessive heating rate ultimately results in lesser resin viscosity, which would make the resin to flow and makes resin to completely soak the carbon fibre surface at the starting phase of the curing process. On the other hand, a lesser viscosity enhances the interfacial bonding and

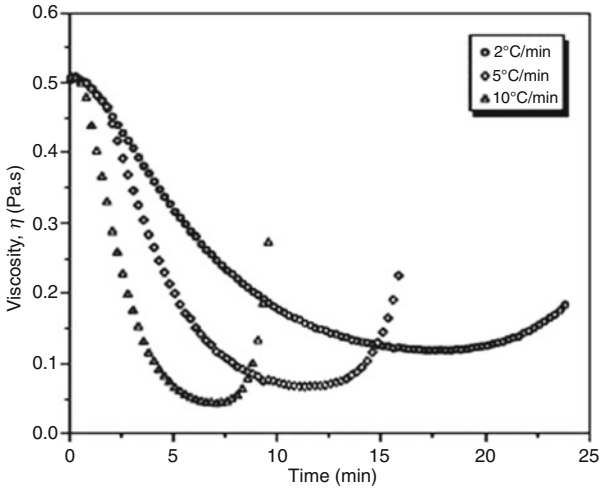

Fig. 13.18 Viscosity versus time at 2, 5, and 10 °C/min for neat LY/HY5052 resin system (Papargyris et al. 2008) (Reproduced with permission from Elsevier Ltd.)

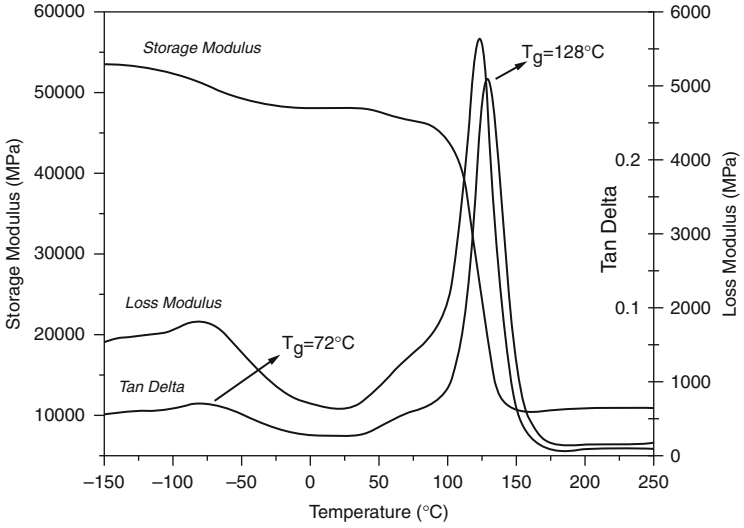

Fig. 13.19 Storage modulus, loss modulus, and tangent delta for the LY/HY5052/carbon composite system cured by conventional thermal RTM (Papargyris et al. 2008) (Reproduced with permission from Elsevier Ltd.)

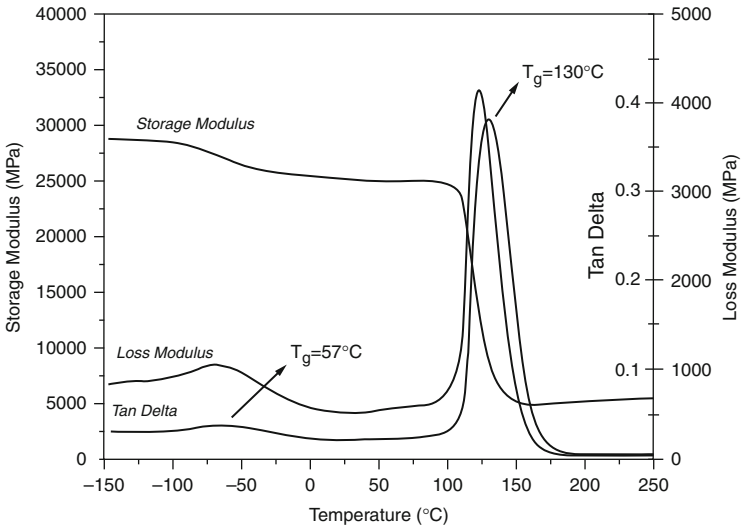

Fig. 13.20 Storage modulus, loss modulus, and tangent delta for the LY/HY5052/carbon composite system cured by microwave RTM (Papargyris et al. 2008) (Reproduced with permission from Elsevier Ltd.)

improves adhesion between the resin and the fibres. Figures 13.19 and 13.20 show the typical DMTA curves at 2 °C/min scan rate and 1 Hz frequency for the thermally and microwave-cured composites. In relation to the average peak values of a-transition, there is no significant difference observed for both types of composites. On the other side, microwave heating shows a higher glass transition temperature (Tg) of 130 ± 1 °C, as opposed to 128 ± 2 °C for those cured thermally. A temperature difference of 15 °C was noticed (average peak values of the lower temperature b-transition) between the two composite types (−72 ± 3 °C and −57 ± 3 °C for the thermally and microwave-cured composites).

Wang et al. (2013) used carboxylic acid functionalized carbon nanotubes (CNTs) to modify epoxy to develop a nanocomposite matrix for hybrid composites. High energy sonication was used to disperse the CNTs in epoxy. RTM process was used to manufacture hybrid multiscale composites specimen which contains less CNTs. The optical microscopy was used to characterize the dispersion quality behavior of CNTs in epoxy. A CNT reinforcement of 0.025 wt% notably increases the glass transition temperatures (Tg) of the hybrid multiscale composites. The fractured surface of failed specimens was examined by SEM.

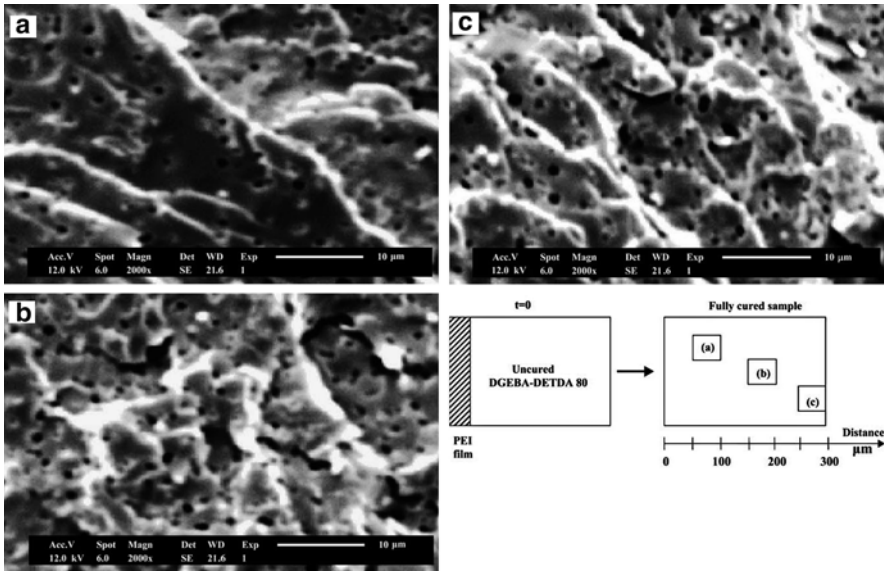

Fig. 13.21 SEM micrographs of fractured specimens of TP/TS blends, obtained from a PEI film embedded in DGEBA–DETDA 80, at different distances from the initial position of the film. Scheme of the position of the observed morphology: (**a**) 0–50 μm, (**b**) 150–200 μm, and (**c**) 250–300 μm (Naffakh et al. 2006) (Reproduced with permission from Elsevier Ltd.)

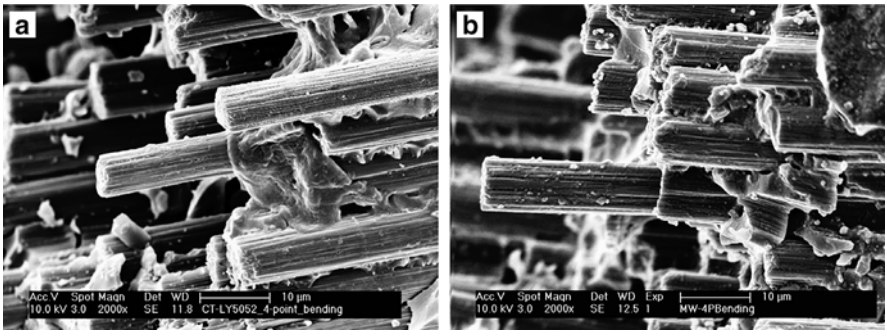

Fig. 13.22 SEM micrographs at the same magnification showing fibre pullout after four-point bending test; (**a**) conventionally cured specimen and (**b**) microwave-cured specimen (Papargyris et al. 2008) (Reproduced with permission from Elsevier Ltd.)

13.7 Morphological Study of RTM Composites

Morphological study can be done by the various available techniques like XRD, SEM, TEM, AFM, etc. SEM can be effectively used for the morphological characterization of natural fibre-reinforced composites. This is the most extensively

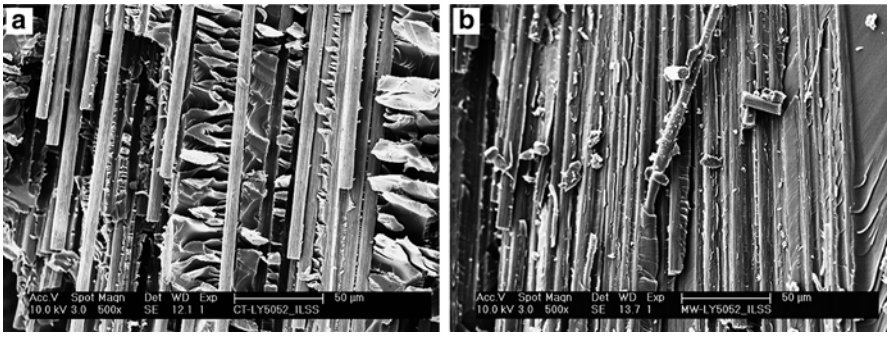

Fig. 13.23 SEM micrographs at the same magnification after interlaminar shear test showing (**a**) clean fibres in conventionally cured specimen and (**b**) fibres coated with resin in microwave-cured specimen (Papargyris et al. 2008) (Reproduced with permission from Elsevier Ltd.)

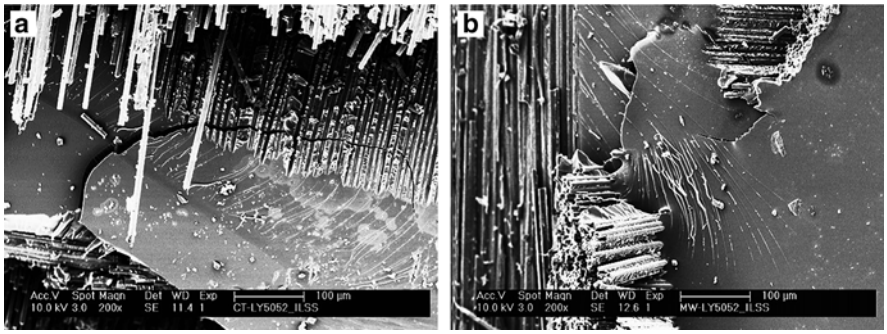

Fig. 13.24 SEM micrographs at the same magnification showing matrix fracture after interlaminar shear test; (**a**) conventionally cured specimen and (**b**) microwave-cured specimen (Papargyris et al. 2008) (Reproduced with permission from Elsevier Ltd.)

used method for the analysis of the surface of composite materials. Figure 13.21 represents the SEM image of "model" blends manufactured from epoxy–amine/thermoplastic films (without glass fibres) noticed at various diffusion lengths. The SEM images showed only one domain size of PEI; this is due to the maximum rate of diffusion of the thermoplastic.

Papargyris et al. (2008) examined the fracture surfaces of composite samples by using SEM. Figures 13.22–13.24 showed the topographic appearance of both types of composites. It can be noticed from Fig. 13.22a, b that the conventional methods show poor interfacial bonding, which can be observed by fracture surface of the composites, and also show broad fibre pullout in contrast to that manufactured by using microwaves. It is clearer in Fig. 13.23a, b, where there is a notable number of clean fibres that appeared in contrast to fibres completely coated with resin. Brittle

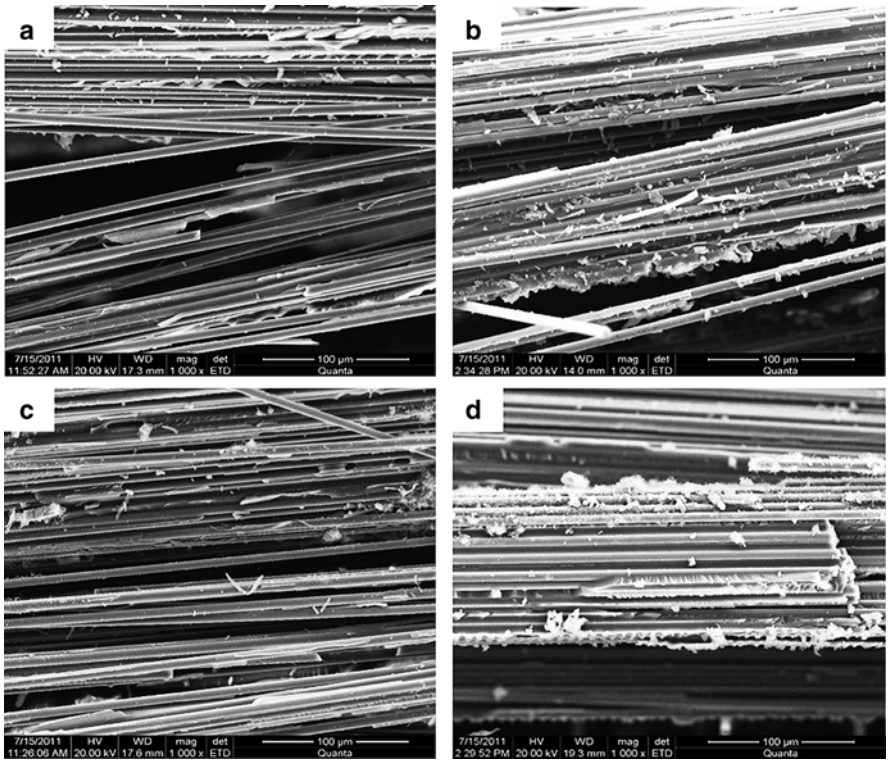

Fig. 13.25 SEM micrographs of fracture surfaces of the hybrid multiscale composites containing various CNTs content: 100 lm scale bar magnification. (**a**) 0 wt%, (**b**) 0.025 wt%, (**c**) 0.075 wt%, and (**d**) 0.1 wt%. (Reproduced with permission from Elsevier Ltd.)

matrix failure sections were also noticed for both types of composites, as presented in Fig. 13.24a, b.

Wang et al. (2013) investigated the fracture surfaces of composites having different amount of CNT content by SEM (Figs. 13.25 and 13.26). Figure 13.25a shows the SEM image of the fracture surface of carbon fibre/epoxy laminates. The fibre pulled out from the matrix surface due to a weak adhesion is confirmed by the smooth fibre surface. Figure 13.26a showed the SEM image of the composites without CNTs. Figure 13.26b showed the composite containing CNTs content of 0.025 wt% which has remarkably different fracture surface. It can be observed from Fig. 13.26b that the continuous reinforcement of carbon fibres was notably smeared with a thin layer of matrix. The combined CNTs were noticed between adjacent carbon fibres as shown in Fig. 13.26b, which ultimately increases the matrix toughness. Figure 13.26c shows the presence of CNTs at the concentration of 0.075 wt%.

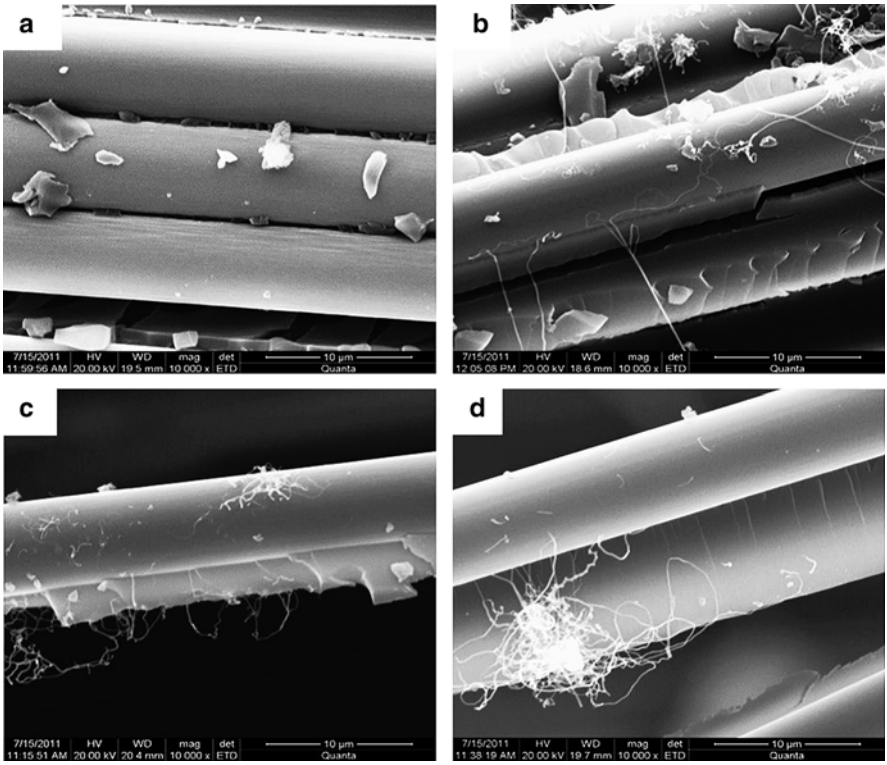

Fig. 13.26 SEM micrographs of fracture surfaces of the hybrid multiscale composites containing various CNTs content: 10 lm scale bar magnification. (**a**) 0 wt%, (**b**) 0.025 wt%, (**c**) 0.075 wt%, and (**d**) 0.1 wt%. (Wang et al. 2013) (Reproduced with permission from Elsevier Ltd.)

13.8 Application of RTM Composites

The applications of the RTM composites generally found in industries are as follows:

(a) In automotive industry, for example, auto body panels, truck air deflector, caravan components, etc.
(b) In consumer products such as dishes antenna, chairs, swim pool panels, bathtub/shower units, solar collectors, etc.
(c) In aerospace and military.
(d) For corrosion resistance applications such as chemical storage tanks, tubes, etc.
(e) Wind turbine blades.
(f) Hollow shapes and complex structures can also be produced by this process.
(g) Big containers and bathtubs are commonly processed through RTM technique.

13.9 Advantages of RTM Composites

The advantages of the RTM composites are as follows:

(a) The part produced by RTM process has good surface finish on both side surfaces of the product.
(b) Any combination or 3D orientation can be achieved by RTM process.
(c) Temperature control device is used for achieving fast cycle time.
(d) The RTM process can be controlled both manually and automatically.
(e) The part made by the RTM process is having uniform thickness throughout.
(f) Low emission achieved during composite fabrication.
(g) Typical dimensional tolerance can be achieved by this process.
(h) The RTM process does not require high injection pressure.
(i) Material wastage is very less as near net shape parts are produced.

13.10 Conclusions

The current chapter focuses on the use of RTM process for the fabrication of the natural fibre-reinforced composite material. The main objective of this chapter is to explore the potential use of RTM process for making polymer composites and also to study the mechanical properties of composites made by the RTM process. Both types of fibres such as chemically treated and untreated can be used for manufacturing of composite materials by considering the various parameters of the said process. The process has good applications in the industry as well, specifically in aerospace industry for making various parts of the aircraft. Wide variety of application of RTM process can also be found for making household equipment. The present chapter also defines the SEM or morphological study of the fractured specimen to understand the fracture mechanism of the composites.

References

Hsiao K-T, Gangireddy S (2008) Investigation on the spring-in phenomenon of carbon nanofiber-glass fiber/polyester composites manufactured with vacuum assisted resin transfer molding. Compos Part A 39:834–842

Laurenzi S, Marchetti M (2012) Advanced composite materials by resin transfer molding for aerospace applications, Compo and Their Prop. Book chapter, Intech open, pp 197–226

Lawrence JM, Hsiao K-T, Don RC, Simacek P, Estrada G, Sozer EM, Stadtfeld HC, Advani SG (2002) An approach to couple mold design and on-line control to manufacture complex composite parts by resin transfer molding. Compos Part A 33:981–990

Leclerc JS, Ruiz E (2008) Porosity reduction using optimized flow velocity in resin transfer molding. Compos Part A 39:1859–1868

Lee G-W, Lee N-J, Jang J, Lee K-J, Nam J-D (2002) Effects of surface modification on the resin-transfer moulding (RTM) of glass-fibre/unsaturated-polyester composites. Compos Sci Technol 62:9–16

Lin L-Y, Lee J-H, Hong C-E, Yoo G-H, Advani SG (2006) Preparation and characterization of layered silicate/glass fiber/epoxy hybrid nanocomposites via vacuum-assisted resin transfer molding (VARTM). Compos Sci Technol 66:2116–2125

Naffakh M, Dumon M, Gerard JF (2006) Study of a reactive epoxy–amine resin enabling in situ dissolution of thermoplastic films during resin transfer moulding for toughening composites. Compos Sci Technol 66:1376–1384

Papargyris DA, Day RJ, Nesbitt A, Bakavos D (2008) Comparison of the mechanical and physical properties of a carbon fibre epoxy composite manufactured by resin transfer moulding using conventional and microwave heating. Compos Sci Technol 68:1854–1861

Pearce NRL, Guild FJ, Summerscales J (1998) An investigation into the effects of fabric architecture on the processing and properties of fibre reinforced composites produced by resin transfer moulding. Compos Part A 29A:19–27

Rouison D, Sain M, Couturier M (2004) Resin transfer molding of natural fiber reinforced composites: cure simulation. Compos Sci Technol 64:629–644

Schmachtenberg E, Schulte zur Heide J, Topker J (2005) Application of ultrasonics for the process control of resin transfer moulding (RTM). Polym Test 24:330–338

Sreekumar PA, Saiter JM, Joseph K, Unnikrishnan G, Thomas S (2012) Electrical properties of short sisal fiber reinforced polyester composites fabricated by resin transfer molding. Compos Part A 43:507–511

Wang B-C, Zhou X, Ma K-M (2013) Fabrication and properties of CNTs/carbon fabric hybrid multiscale composites processed via resin transfer molding technique. Compos Part B 46:123–129